

# GCS: Generalized Cache Coherence For Efficient Synchronization

Yanpeng Yu    Seung-seob Lee    Anurag Khandelwal    Lin Zhong  
Yale University

## Abstract

We explore the design of scalable synchronization primitives for disaggregated shared memory. Porting existing synchronization primitives to disaggregated shared memory results in poor scalability with the number of application threads because they layer synchronization primitives atop cache-coherence substrates, which engenders redundant inter-core communications. Substantially higher cache-coherence latency ( $\mu\text{s}$ ) with substantially lower bandwidths in state-of-the-art disaggregated shared memory designs amplifies the impact of such redundant communications and precludes scalability.

In this work, we argue for a co-design for the cache-coherence and synchronization layers for better performance scaling of multi-threaded applications on disaggregated memory. This is driven by our observation that synchronization primitives are essentially a generalization of cache-coherence protocols in time and space. We present GCS as an implementation of this co-design. GCS employs wait queues and arbitrarily-sized cache lines directly at the cache-coherence protocol layer for temporal and spatial generalization. We evaluate GCS against the layered approach for synchronization primitives — the pthread implementation of reader-writer lock — and show that GCS improves in-memory key-value store performance at scale by 1 – 2 orders of magnitude.

## 1 Introduction

Scalable and low-latency synchronization primitives such as locks [1–14] are crucial for the performance of multi-threaded applications. In multi-core CPU architectures, lock-based synchronization primitives are built atop an efficient hardware-based cache coherent substrate, which provides building blocks in the form of atomic memory instructions [15–17] on a unit of cache data, i.e., a cache line.

With the end of Moore’s Law and the consequent challenges in scaling DRAM technologies [18] in a single server, recent years have seen a push towards rack-scale compute-memory disaggregation [19–33], where server resources are physically decoupled into compute and memory blades connected via a high-speed network fabric, with the compute blades equipped with a small amount of DRAM as a cache. Recent efforts have also focused on enabling cache-coherent shared memory abstractions over them for application transparency. It stands to reason that the lock primitives developed for multi-core architectures could be ported to cache-coherent substrates atop disaggregated memory.

Unfortunately, the unique characteristics of disaggregated architectures make their cache-coherent substrates fundamentally inadequate for an efficient realization of atomic instructions that traditional lock primitives have leveraged. In par-

ticular, while inter-cache communications for cache coherence in multi-core and NUMA architectures observe latencies around 20–100 ns and operate over a bandwidth upwards of 500 Gbps, those for disaggregated architectures see latencies of 5–10  $\mu\text{s}$  while the bandwidth drops to 100 Gbps, even with RDMA [33–35]. As such, even scalable lock primitives layered over state-of-the-art coherent substrates for disaggregated memory [33, 36] observe poor performance scaling (§2).

To address the overhead, recent approaches have proposed efficient standalone lock services [37–40] that bypass the shared memory layer altogether. While these approaches achieve better performance scaling than layered approaches, they do not support applications designed for shared memory and still require accessing two separate services — lock and shared memory — resulting in sub-optimal performance.

This raises the question: *Is it possible to design a lock-based synchronization framework on shared disaggregated memory that is scalable and performant?* We answer the question in the affirmative with a principled redesign of lock-based synchronization, drawing on two key observations.

First, we find that the key reason behind the poor scalability and performance of shared memory locks on disaggregated memory lies in the layering of lock primitives atop cache coherence: much of the communications incurred across the two layers are redundant (§2). In fact, a closer inspection (§3) reveals a far more direct relationship between lock-based synchronization and coherence, i.e., lock-based synchronization is essentially a *generalization* of cache coherence in *time* and *space*:

- **Temporal generalization.** Cache coherence protocols guarantee SWMR semantics, i.e., single-writer, multi-reader semantics, for the duration of a single instruction. In contrast, reader-writer lock-based synchronization requires this atomicity property for an arbitrary number of instructions — specifically, the critical section.
- **Spatial generalization.** Similarly, cache-coherence protocols ensure atomicity at a cache line granularity (64B in most CPU architectures), while reader-writer locks typically require atomicity for shared states of arbitrary sizes.

An extension of existing cache-coherence protocols that supports these temporal and spatial generalizations would eliminate the redundant communications seen in a layered design, enabling more scalable and performant lock-based synchronization. Moreover, co-designing synchronization with coherence also enables opportunities for other optimizations, e.g., caching lock and shared data until explicitly invalidated, pipelining movement of shared data (i.e., the cache line in co-

herence protocols) with lock acquisition, etc., enabling further improvement in application performance.

Second, while communications in disaggregated systems interconnects do observe higher latencies and lower bandwidths, making the overheads of the layered design far more pronounced than in traditional multi-core architectures, they are also inherently more flexible to program. We argue that the same flexibility can enable the temporal and spatial generalization of coherence protocols described above.

We incorporate the above insights into a generalized cache-coherence protocol for lock-based reader-writer synchronization to avoid redundant network communications in a layered design. Our generalized cache coherence builds on directory-based MSI protocol [41], and uses two key ideas to achieve this:

- **Wait queues for temporal generalization.** MSI-based cache coherence only guarantees that a cache line requested by a thread (for reads or writes) will be held in the requestor’s cache for a single instruction — a subsequent read or write requests from other threads *invalidate* the cache line on the old requestor. To allow a requestor to hold the cache line for more than one instruction, generalized cache coherence prevents other requestors from invalidating the cache line until the original requestor explicitly releases it; the other requestors are instead recorded in a wait queue, and their execution is suspended until it is their turn to access the cache line<sup>1</sup>. Note that the use of wait queues for synchronization is not new; however, our approach differs in embedding them at the *cache-coherence layer*.
- **Arbitrarily-sized cache lines for spatial generalization.** Spatial generalization is relatively straightforward — while directory-based MSI cache-coherence protocol tracks a single fixed-sized cache line at each directory entry, our generalization simply tracks a list of arbitrarily-sized memory regions per directory entry. During invalidations, all of the shared regions tracked by the directory entry are removed from the target cache. This allows threads to achieve atomic access to arbitrary-sized shared regions for the duration of their critical section.

This essentially transforms directory entries in the MSI protocol into lock entries for synchronizing shared state.

We present GCS as an implementation of generalized cache coherence atop MIND [33]’s in-network cache coherence for performance and scalability, along with a number of additional optimizations. In order to ensure feasibility, GCS places the minimal required state and logic associated with coherence in the programmable network switch to work around the switch’s limited resources, while delegating much of it — including the wait queue — to the compute blades. Since the shared

<sup>1</sup>The order in which requestors get to access the cache line can be determined by flexible policies and has been extensively studied in prior work, e.g., FIFO, random, priority order, etc.

memory regions to be accessed by a critical section are already tracked by the directory entries, GCS proactively pipelines the movement of corresponding data with lock acquisition to minimize data access latency during the critical section.

GCS enables complete transparency for legacy shared memory applications by wrapping its generalized cache-coherence protocol in a POSIX-compliant reader-writer lock API. Since POSIX APIs do not require threads to explicitly specify what shared memory regions are protected by a lock, GCS can *infer* them by tracking shared memory regions accessed during a critical section protected by a specific lock. GCS also provides APIs to let programmers explicitly specify memory regions to be protected by a lock during lock initialization for more accurate tracking — indeed, this programming model is increasingly common in modern languages like Rust. Our evaluation shows that GCS enables scalable and high-performance lock-based reader-writer synchronization on disaggregated memory. Specifically, compared to a layered approach for lock primitives — the `pthread` implementation of reader-writer lock — on a disaggregated cluster, GCS improves the throughput of a in-memory key-value store by 19 – 331× for different workloads.

## 2 Motivation

We begin with a brief background on cache coherence and synchronization (§2.1), and then demonstrate the inefficiency of a layered design for the two (§2.2).

### 2.1 Background

**Cache coherence.** Most modern CPU architectures use either *snoop-based* or *directory-based* cache coherence protocols. We focus on directory-based ones in this work because most systems of NUMA-scale or larger (including proposals for disaggregated memory [33, 36]) use them for their scalability.

Directory-based protocols employ a logically centralized cache directory to track the state of basic memory unit — typically referred to as a cache line — present in the distributed caches. The state at the directory includes the list of caches that currently hold the cache line (i.e., the “sharer list”), and what permissions they have. When any cache intends to acquire a cache line, it first contacts the directory, which subsequently notifies other caches in the sharer list about the transition and coordinates any subsequent data movement.

Consider a simple directory-based MSI protocol, where each cache line can be in one of the three permissions:

- **M** or modified, indicating a single cache has *exclusive* read and write permissions for the cache line,
- **S** or shared, where multiple caches have *shared* read permission to the cache line, and,
- **I** or invalid, i.e., the cache line is not present in any cache.

Fig. 1 shows an example with a single cache line at address `0x0A`, a cache directory, and two nodes —  $N_1$  and  $N_2$ . The

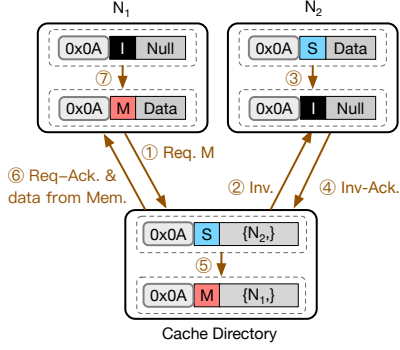


Fig. 1: Directory-based MSI Protocol (§2.1).

cache line is initially cached at  $N_2$  with **S** permission.  $N_1$  then requests the same cache line with **M** permissions from the cache directory (①). The directory looks up the sharer list for the cache line and contacts  $N_2$ , the current holder of the cache line. Specifically, the cache directory must *invalidate* the cache line at  $N_2$ , since  $N_1$  needs exclusive access to it (②). After removing the cache line from its own cache (③),  $N_2$  informs the directory (④), which then updates the cache line’s permissions to **M**, marks  $N_1$  as the only sharer in the sharer list (⑤) and sends  $N_1$  an acknowledgment along with the corresponding cache line data (⑥).  $N_1$  subsequently proceeds with its access to the cache line (⑦).

While the above example demonstrates the execution for an **S**→**M** transition in cache permission, other transitions are either similar or even simpler. Specifically, **M**→**M** and **M**→**S** transitions require similar invalidations for the node initially holding the cache line with **M** permission. On the other hand, **S**→**S**, **I**→**S** and **I**→**M** transitions require no invalidations, only updates to the sharer list and permissions for the cache line at the directory, while the data can directly be fetched from main memory.

**Lock-based Synchronization.** Locks are the foundation to modern synchronization solutions for large-scale shared memory systems. The pursuit of high performance locks has yielded numerous scalable algorithms, like the MCS lock algorithm [4]. Consider a number of threads running on separate CPU cores, each with its own private cache, trying to acquire the same lock. The MCS lock queues requestor threads, with each queue entry including two pieces of information — an atomic flag (*waiting*), which tracks whether the requestor is waiting on the lock or not, and a pointer to the next queue entry (*next*). The requestor at the head of the queue holds the lock (i.e., its *waiting*=*false*), while other requestors spin locally on their queue entry — specifically, the *waiting* flag, which is set to *true*. To release the lock, the lock holder (at the head of the queue) simply sets the *waiting* flag for the requestor next in the queue to *false*. Since all inter-core communications are restricted to neighboring requestors in a fixed order, this limits MCS lock’s inter-core communications per lock acquisition and release to a constant, independent of the

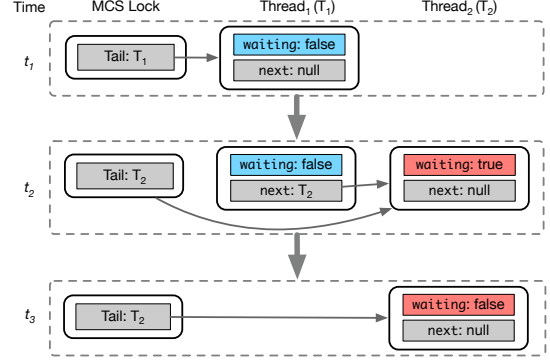


Fig. 2: MCS-Lock Operation (§2.1).

number of requestors.

The example in Fig. 2 illustrates the operation of the MCS lock. At time  $t_1$ , thread  $T_1$  acquires the lock as it is the only requestor in the queue. At time  $t_2$ , thread  $T_2$  is added to the queue, and polls at its private *waiting* flag until the value becomes *false*. At time  $t_3$ , thread  $T_1$  hands over the lock to  $T_2$  by setting  $T_2$ ’s *waiting* as *false*. Thread  $T_2$  then detects the updated *waiting* flag and proceeds to its critical section.

## 2.2 Inefficiencies due to a Layered Design

We find that well-optimized lock algorithms like MCS lock still trigger redundant inter-core communications via cache-coherence traffic, resulting in additional lock handover latency and interconnect bandwidth consumption. In the Fig. 2 example, the lock ownership transition from thread  $T_1$  to  $T_2$  at time  $t_3$  triggers three sequential cache-coherence transactions in the MSI protocol:

1. To find the next requestor, thread  $T_1$  fetches the cache line containing the *next* field within its queue entry with **S** permission since it had previously been cached by thread  $T_2$  with **M** permission at time  $t_2$  — this **M**→**S** transition triggers an invalidation, as discussed in §2.1;
2. When thread  $T_1$  updates  $T_2$ ’s *waiting* to *false*, it must fetch the cache line containing the *waiting* flag with **M** permission, since it had previously been cached by thread  $T_2$  with **M** permission at time  $t_2$  — again, this **M**→**M** transition triggers an invalidation; and,
3. Finally, thread  $T_2$  can only detect that it owns the lock now after it reads its own queue entry’s *waiting* flag. This requires fetching the corresponding cache line back with **S** permission since it was just cached by thread  $T_1$  in step 2. This **M**→**S** transition triggers yet another invalidation.

In addition to the three coherence transactions described above, adding thread  $T_2$  to the queue triggers two more coherence messages. While the delays caused by these messages can be subsumed by the time that thread  $T_2$  waits for the lock, the traffic still contributes to inefficient use of the inter-core interconnect bandwidth. As such, the MCS lock incurs 5 coherence transactions for each lock handover, with 3 of them in the critical path.

The inefficiency is not limited to the MCS lock but fundamental to all scalable synchronization algorithms. Specifically, scalable synchronization algorithms must partition the lock’s state across multiple cache lines to restrict inter-core communications (*e.g.*, the tail pointer and core-private queue entries in MCS lock). This unavoidably causes multiple sequential accesses to the cache lines containing the partitioned lock state for every synchronization operation, each of which triggers its cache-coherence transaction. We note that these inefficiencies mainly stem from the layering of the lock algorithm atop the shared memory abstraction, which uses cache coherence as a black box. A synchronization mechanism that is co-designed with the cache-coherence protocol can (§3) — and, as we demonstrate in §5, does — circumvent these inefficiencies. In particular, we show that the acquisition and release of reader-writer locks can be facilitated with a single coherence transaction each.

It is understandable why such a co-design has not been explored in the past — given the low-latency, high-bandwidth cache-coherence substrates in multi-core and NUMA architectures, the additional inefficiency is all but negligible. As such, much of prior work has focused on improving the scalability of such locks, without considering the latency and number of interconnect messages triggered during their acquisition and release. However, with each inter-core communication incurring several microseconds of delay and consuming a non-trivial fraction of the interconnect bandwidth in disaggregated architectures, this inefficiency often results in significant application performance degradation.

### 3 Co-designing Cache-coherence with Reader-Writer Synchronization

We now describe our approach that eliminates the inefficiencies of the layering reader-writer synchronization atop cache coherence via a *co-design* of the two layers. Our key enabling observation is that reader-writer synchronization is, in fact, a *generalization* of cache coherence. We describe the required extensions to the cache-coherence protocol for achieving such a generalization in §3.1 and demonstrate how standard synchronization interfaces can be realized via our generalized cache-coherence protocol in §3.2. We conclude by describing additional optimizations enabled by our generalization for reader-writer synchronization in §3.3.

#### 3.1 Generalized Cache-coherence

Fundamentally, both cache coherence and reader-writer synchronization strive for the same goal — single-writer, multi-reader (SWMR) semantics over some shared state. Under SWMR semantics, at any point in time, either a single entity that intends to modify the shared state has *exclusive* access to it or multiple entities that intend to only read from the state without modifying it, have *shared* access to it. SWMR semantics is the building block for ensuring correctness in layers above, *e.g.*, memory consistency for cache coherence,

and data consistency in synchronization. While consistency models vary across both layers and even within each layer, SWMR is at the heart of both.

The key distinction between cache coherence and synchronization, however, stems from the temporal and spatial granularity at which SWMR semantics are enforced. In particular, cache-coherence protocols ensure these semantics at a single instruction granularity (in time) and at a fixed cache line granularity (in space). In contrast, reader-writer synchronization strives for these semantics at arbitrary instruction count (typically referred to as a critical section) and arbitrary data size granularities. It is easy to see, then, that reader-writer synchronization is simply a generalization of cache coherence in time and space. Historically, cache coherence has been implemented in hardware across multi-core caches and is invisible to software, while synchronization has been implemented in software. As such, the latter is forced to recreate its generalized SWMR semantics atop the former (§2.2).

With programmable cache-coherence substrates, however, we can realize a generalized cache-coherence protocol capable of directly supporting reader-writer synchronization. We illustrate the design for the same next (§3.1.1, §3.1.2), using MSI cache-coherence protocol as our base protocol. Note that while similar generalizations are possible for more complex protocols (*e.g.*, MESI [42], MOSI [43], or MOESI [44]), we focus on the MSI protocol for its simplicity.

##### 3.1.1 Temporal Generalization

As we saw in §2.1, a directory-based cache-coherence protocol ensures SWMR semantics by tracking the permission of the requested cache line — **M**, **S** or **I**. If an instruction’s execution at one node (*e.g.*, a CPU core in multi-core architecture or a compute blade in disaggregated architectures, etc.) requests a cache line with specific permission, the protocol triggers a transaction that makes the cache line available with that permission to that instruction immediately. For instance, in Fig. 1, the protocol provides the cache line to node  $N_1$  with **M** permission via a transaction that (i) invalidates the cache line at  $N_2$ ’s cache, and (ii) updates the sharer list and permission for the cache line at the directory.

To enable the temporal generalization of the protocol, where a node can hold the cache line with certain permission for an arbitrary number of instructions (critical section), we must be able to *delay* other nodes from acquiring the cache line immediately in some cases. Specifically, other nodes should be able to acquire the cache line only after the first node explicitly releases it, marking the end of its critical section. A natural way to enable such deferred cache line (and associated permission) transfers is by enqueueing such requests in a *wait queue*, and dequeuing the request only when the first node releases the cache line. This is akin to wait queues used in synchronization primitives, except the queue is embedded within the cache-coherence protocol layer.



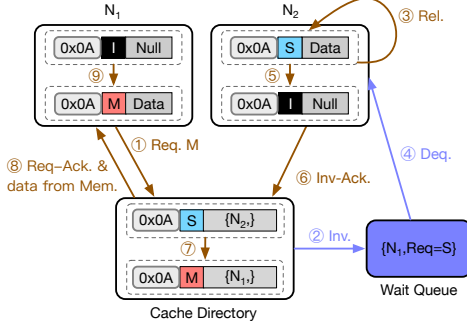


Fig. 3: Temporal generalization with wait queues (§3.1.1).

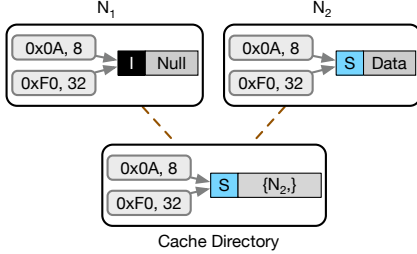


Fig. 4: Spatial generalization with shared-memory lists (§3.1.2).

Fig. 3 demonstrates how a wait queue can enable temporal generalization for the same example in Fig 1. The target cache line is initially cached at  $N_2$  with  $S$  permission. Subsequently,  $N_1$  requests the same cache line with  $M$  permission from the cache directory (①). The directory looks up the current cache line permission ( $S$ ) and sharer list ( $\{N_1\}$ ), realizing that the request requires  $N_2$  to relinquish the cache line via invalidation. In contrast to standard MSI protocol execution, the directory defers the invalidation and instead enqueues  $N_1$ 's request in a wait queue associated with the cache line (②). Only when  $N_2$  finishes its critical section and voluntarily releases the cache line (③) is the request dequeued (④) and the invalidation performed at  $N_2$  (⑤). The remainder of the cache-coherence transaction proceeds similarly to the standard MSI protocol —  $N_2$  informs the directory (⑥), which updates the cache line's permission to  $M$  and marks  $N_1$  as the only sharer (⑦), and sends  $N_1$  an acknowledgment along with the cache line data (⑧).

As with cache coherence, other cache line and permission transfers are either similar or simpler. Specifically,  $M \rightarrow M$  and  $M \rightarrow S$  transfers require similar deferred invalidations by enqueueing the transfer requests at the wait queue, until the node initially holding the cache line with  $M$  permission explicitly releases it. Moreover,  $S \rightarrow S$  transfers do not require enqueueing the request since multiple readers can hold the cache line simultaneously under SWMR semantics. Similarly,  $I \rightarrow S$  and  $I \rightarrow M$  transfers also do not require enqueueing requests, since no node has the cache line to begin with.

Note that where the wait queue is placed does not matter for correctness but does for performance. We defer the discussion on how our implementation navigates various tradeoffs for wait queue placement to §4.2.

Language	Code Snippets
C (pthread)	<pre>pthread_rwlock_t l; pthread_rwlock_init(&amp;l); // Initialize lock pthread_rwlock_wrlock(&amp;l); // Critical section for write lock pthread_rwlock_unlock(&amp;l); pthread_rwlock_rdlock(&amp;l); // Critical section for read lock pthread_rwlock_unlock(&amp;l);</pre>
Rust	<pre>struct Data {     key: u64,     val: u64 } // Initialize lock let l = RwLock&lt;Data&gt;::new(Data::default()); { // Critical section for write lock     let mut w = l.write().unwrap();     (*w).key = 42;     (*w).val = 42; } { // Critical section for read lock     let r = l.read().unwrap();     assert_eq!((*r).key, 42)     assert_eq!((*r).val, 42) }</pre>

Table 1: Reader-writer synchronization in C and Rust. (§3.2).

### 3.1.2 Spatial Generalization

Unlike coherence protocols that track permissions for a fixed-size cache line, synchronization primitives need to preserve SWMR semantics for arbitrary amounts of shared state. The shared state may be fragmented, and may even be empty. Fortunately, directory-based cache-coherence protocols provide a convenient way of tracking multiple shared memory locations of arbitrary size — directly within the directory entries. Specifically, in our generalized cache-coherence protocol, instead of tracking a single fixed-size cache line, each directory entry tracks multiple shared memory regions of arbitrary size. To enable this, each directory entry stores a list of  $(m_i, s_i)$  pairs, where  $m_i$  corresponds to the base address of a shared memory region and  $s_i$  its size in bytes. For standard cache coherence, this simply reduces to a single entry of 64B.

Fig. 4 shows our spatial generalization for the same example as Fig. 3. The directory tracks two shared memory locations:  $\{(0x0A, 8), (0xF0, 32)\}$ . The protocol execution is identical to the description in §3.1.1, except the invalidation step ⑤ now requires  $N_2$  to remove two memory regions of different sizes from its cache, and in step ⑧, the directory sends  $N_1$  the data corresponding to both regions along with the acknowledgment. Again, we defer a discussion of the tradeoffs stemming from an architecture-specific implementation of the shared memory list to §4.3.

## 3.2 Supporting Synchronization Interfaces

While §3.1 described how the directory-based MSI cache-coherence protocol can be generalized, we now describe how various popular synchronization interfaces can leverage the generalized protocol for efficient performance scaling.

**Synchronization in C (pthread).** Arguably, the most popular

interface for reader-writer synchronization in multi-threaded applications is the `rwlock` in the POSIX threads (`pthread`) library interface (Table 1 (top)). The lock is acquired in either write or read mode via the `pthread_rwlock_wrlock` or `pthread_rwlock_rdlock` function, respectively, and unlocked via the `pthread_rwlock_unlock` function. In generalized cache coherence, the cache line simply tracks the lock variable (1). Acquiring the lock in write or read mode triggers a request for the cache line with **M** or **S** permission, respectively. Finally, releasing the lock triggers releasing the cache line in the generalized cache-coherence protocol.

Note that the POSIX API does not explicitly specify the shared memory that will be accessed in the critical section. Since the lock already ensures SWMR semantics for any thread in the critical section, the shared state in this region can directly be accessed via shared memory without violating correctness, albeit with unnecessary coherence traffic for the corresponding accesses. Instead, our adaptation to the POSIX API *infers* the shared memory regions being accessed during the critical section by simply tracking accesses to them between lock acquisition and release. This only needs to be done the first time any thread enters the critical section, and can be added to the cache line’s shared memory list at the directory — all subsequent acquisitions and releases of the lock directly trigger the invalidation of these regions as needed.

**Synchronization in Rust (`std::sync`).** Table 1 (bottom) shows the operation of Rust’s `std::sync::RwLock`. Unlike `pthread`’s reader-writer synchronization, `RwLock` explicitly takes the state being protected by the lock (a `Data` object in our example) as an argument. This makes adapting generalized cache coherence to `RwLock` even simpler and more efficient. In particular, while the cache line still tracks the lock variable, but its directory entry is initialized with the shared memory list containing the address and size of the shared object (*e.g.*, the protected `Data` object in the shown example). Lock acquisition and release, on the other hand, proceed similarly to `pthread`, as described above.

### 3.3 Cache-coherence Optimizations

As one would expect, our generalized cache-coherence protocol achieves performance scalability since it avoids redundant communications observed in a layered design (§2.1). Indeed, our analysis of the MCS lock workflow in §2.2 showed that the critical path in reader-writer synchronization — the lock handover to the next requestor — requires three sequential cache-coherence transactions. In contrast, our generalized cache-coherence protocol provides the same SWMR semantics as MCS locks but with the lock handover requiring a single cache-coherence transaction (§3.1.1).

Interestingly, our generalized cache coherence also has the fortunate side-effect of inheriting optimizations from traditional cache-coherence protocols. These optimizations can further reduce overheads in many common scenarios seen in reader-writer synchronization, as we demonstrate below.

**Acquiring shared state along with lock.** As shown in §3.2, popular reader-writer synchronization interfaces (*e.g.*, `pthread`) decouple lock acquisition from fetching the shared data associated with the lock, which results in additional delay and coherence traffic in placing the corresponding shared state in the requestor’s cache. Although modern languages like Rust address this issue to some extent by coupling the shared state with the lock, the layering of lock atop cache coherence provides no guarantee that the underlying hardware will fetch both together. Moreover, since cache line sizes are limited to 64B in traditional architectures, placing any fragmented shared state, or state of size greater than 64B in the requestor’s cache requires multiple cache-coherence transactions. In contrast, our generalized protocol performs the acquisition of the shared state (cache line) and the lock (access permission) in a single communication, akin to traditional cache coherence. Moreover, with our spatial generalization, we can place all shared state protected by a lock (of any size and with any amount of fragmentation) within the requestor’s cache, in a single cache-coherence transaction.

**Exploiting temporal locality for locks.** In traditional cache-coherence protocols, once a cache line is placed in a requestor’s cache, it remains there until it is invalidated, in order to exploit the temporal locality of data accesses. By extending such protocols, our generalized cache coherence inherits the same optimization — both the lock and the shared state associated with it remain in the requestor’s cache until it is explicitly invalidated by another request. Interestingly, optimized lock algorithms in multi-core architectures do exploit a similar optimization, wherein threads running on the same core can enter the critical section multiple times without communicating with other cores, as long as threads on other cores do not attempt to acquire the same lock. However, standalone lock services [37–40] cannot exploit such an optimization because their locks are decoupled from shared memory.

## 4 GCS: A Generalized Cache-coherence Implementation atop Disaggregated Memory

We present GCS as an implementation of generalized cache coherence on a disaggregated shared memory architecture. We begin with a brief background on MIND, the shared disaggregated memory platform that GCS builds on (§4.1), followed by design details on how we incorporate wait queues (§4.2) and shared memory lists (§4.3) within MIND’s programmable cache-coherence substrate.

### 4.1 Disaggregated Shared Memory Platform

While generalized cache coherence can be realized on any flexible cache-coherence substrate, GCS focuses on disaggregated architectures, since their higher latencies and lower bandwidths present a pressing need for more efficient and scalable synchronization primitives (§2.2).

A recent approach for rack-scale disaggregated shared memory, MIND [33], realizes an efficient directory-based

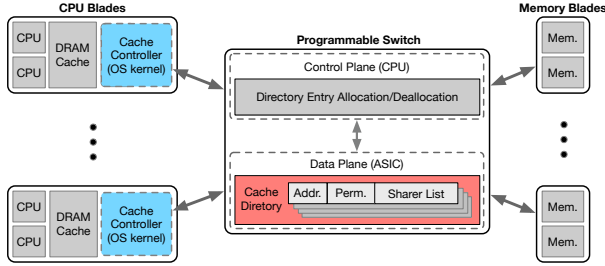


Fig. 5: **MIND Architecture** (§4.1). GCS’s modifications are confined to the cache controller (blue) and the cache directory (red).

MSI cache-coherence substrate by leveraging in-network processing. We decided to implement atop MIND for three reasons. First, since much of the cache-coherence logic is implemented in hardware, it observes better scalability and lower latency relative to software-based alternatives. Second, since MIND is implemented across P4 programmable network hardware and kernel software, it is extensible enough to support our cache-coherence generalizations. Finally, MIND is publicly available [45].

**MIND Architecture.** Fig. 5 shows MIND’s rack-scale architecture for cache coherence. It comprises compute and memory blades connected via a programmable network switch. Each compute blade is equipped with a small amount of DRAM used as a cache — if an application accesses a cache line (page granularity in MIND) not present in the DRAM cache, it triggers a page fault. The fault handler initiates coherence transactions via cache controller logic implemented in the kernel — it sends out requests for the cache line with **S** or **M** permissions for faulting **LOAD** or **STORE** operations, respectively. The programmable switch implements the cache directory, issuing invalidations to relevant compute blades and updating its local cache line state (cache line permissions and the sharer list) as necessary. Invalidation requests are handled by in-kernel cache controller logic at compute blades, which removes the cache lines from the cache. In case none of the compute blades have the cache line in their cache, it is fetched from disaggregated memory via RDMA. While MIND implements additional components for realizing a complete virtual memory subsystem, we omit their details since they are unnecessary for understanding GCS’s implementation.

While MIND’s realization of cache coherence across programmable network hardware and kernel software affords both performance and flexibility, the in-network implementation of its cache directory also imposes resource constraints on extensions to the directory. Specifically, our generalizations to cache-coherence protocol (§3.1) require additional storage and processing logic for every cache line, ideally at the directory. However, the programmable switch ASIC only has a few megabytes of on-chip memory and can only support a few cycles of computation per packet [33], much of which is already used up by MIND’s realization of virtual memory components (including cache coherence). As such,

GCS’s implementation atop MIND must navigate various tradeoffs between feasibility and efficiency for realizing the wait queues and shared memory lists, as we discuss next.

## 4.2 Implementing the Wait Queue

At a first glance, the cache directory appears to be a good location for the wait queue — its central location simplifies consistency issues for concurrent updates and makes it accessible from any compute blade in half a round-trip. However, the queue requires a non-trivial amount of already scant storage and processing resources for enqueue and dequeue operations. On the other hand, while a shared memory realization suffers none of the resource constraints, it requires additional coherence traffic — against main goal of eliminating unnecessary network traffic for better performance.

Placing the wait queue at the compute blades circumvents both the resource limitations of a switch-based realization and the performance overheads of a shared memory realization. However, one challenge that remains is maintaining consistency for the queue when multiple compute blades concurrently want to enqueue or dequeue requests on a particular cache line’s queue. Specifically, if multiple compute blades currently hold the cache line, then how do we maintain a consistent view of the queue across them in the presence of concurrent requests? Moreover, the set of compute blades that hold the cache line can change over time, necessitating a change of ownership for the corresponding wait queue.

Fortunately, SWMR semantics permit a simple solution to both problems. Since only a single writer (i.e., a thread requesting the cache line with **M** permission) can hold a cache line at a given time, only one blade (the one hosting the writer) needs to track the queue at that time. If the cache line moves from one writer to another, the queue moves with it. While multiple readers (i.e., threads requesting the cache line with **S** permission) can hold a cache line concurrently, placing the cache line at additional readers does not require enqueueing requests (§3.1.1). As such, no reader needs to maintain a queue — or more precisely, no queue needs to be tracked for a cache line that is only requested by readers. However, if a cache line initially held by multiple readers is subsequently requested by a writer, a wait queue must be created for it. Fortunately, this queue can simply be created and maintained at the blade that hosts the corresponding writer.

In summary, the wait queue for a cache line either (i) does not exist (if there are no writers requesting the cache line), (ii) is maintained at the compute blade hosting the current writer (if the cache line is held by a writer), or, (iii) is maintained at the compute blade hosting the next writer that will get the cache line (if the cache line is held by one or more readers). Since only one blade holds the queue for a cache line (“queue holder”) at any given time, it simplifies consistency for the queue. Moreover, the cache directory at the switch only needs to track which compute blade is the current queue holder for each cache line, in order to forward corresponding access

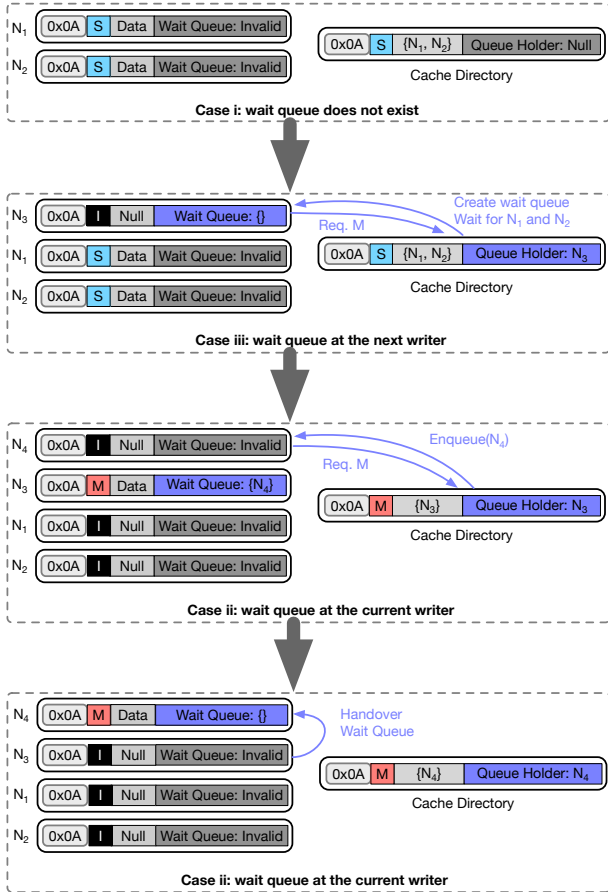


Fig. 6: GCS queue holders under different scenarios. When there are only readers and no writers, the wait queue does not exist (Case i). As soon as a writer appears, the wait queue is created and held by the next waiting writer  $N_3$  (Case iii). Once the readers release the lock,  $N_3$  becomes the current writer (Case ii). When another writer  $N_4$  acquires the lock, the wait queue is transferred to it (Case ii).

requests to it. The queue holder then enqueues the request until the cache line is voluntarily released. Fig. 6 summarizes the various possible locations and transferring of the queue.

**Consistency during queue transfers.** A subtle consistency issue can occur when the cache directory forwards an access request to a queue holder that is in the process of transferring the queue to another compute blade. In particular, should such a request be processed by the original queue holder or the next one? To resolve such ambiguities, GCS employs a versioning mechanism to ensure the queue transfer occurs *atomically*, effectively ensuring that an access request is never forwarded to a compute blade in the middle of a queue transfer. Specifically, the directory maintains a version number for each cache line that tracks the number of access requests it has forwarded to the queue holder, while the queue holder maintains its own version number to track the number of access requests it has received from the directory. A wait queue transfer is approved by the switch only if the queue holder’s version number matches that of the directory, ensuring that all access

requests forwarded by the directory must have been processed at the queue holder before it initiated the transfer. If the switch denies a queue transfer, the queue holder reattempts the queue transfer after receiving the notification from the switch. On a successful transfer, the version numbers at both the switch and the queue holder are reset to zero.

### 4.3 Implementing the Shared Memory List

Unlike the wait queue, the shared memory list is embedded within directory entries in our generalized cache-coherence protocol (§3.1.2). This is because invalidations are triggered by the directory (which has the sharer list), and so must be aware of the memory regions that need to be invalidated. While the processing logic for the list itself is not complex, an unbounded list of fragmented memory regions cannot be held in the programmable switch’s on-chip memory. Instead, we modify MIND’s memory allocator at the control plane to only allocate contiguous memory regions for shared memory protected by a lock. This reduces the shared memory list to a single  $(m, s)$  tuple tracking the region’s base address and size, and permits a feasible and performant realization of spatial generalization at the switch ASIC in GCS.

## 5 Evaluation

We evaluate GCS to demonstrate its performance scaling for real-world multi-threaded applications on disaggregated memory (§5.1), understand the contributions of its optimizations (§5.2) and study the impact of temporal and spatial generalization on its performance (§5.3).

**Compared systems.** We compare GCS against reader-writer synchronization primitives layered atop cache coherence. We use `pthread_rwlock` [46] implemented atop MIND for the latter since it is one of the most widely used reader-writer lock, exploiting the `futex` [47] wait queue service provided by the Linux kernel for performance scalability. GCS itself also adapts the generalized cache-coherence protocol to the same `pthread_rwlock` interfaces, to maintain parity across the two approaches in terms of supported applications.

**Evaluation setup.** We use a cluster with five servers connected via a programmable switch to deploy GCS atop MIND. The switch has a 32-port 6.4 Tbs Tofino programmable switch ASIC. One of the servers is equipped with two 18-core Intel Xeon processors, 384GB memory, and four Mellanox CX-5 100 Gbs NICs, and is used to host a single MIND memory blade VM. The remaining four servers are equipped with two 12-core Intel Xeon processors and two Mellanox CX-5 100 Gbs NICs each, and host two MIND compute blade VMs per server, each with 512MB DRAM. MIND supports the transparent execution of multi-threaded shared memory applications — our implementation of GCS preserves this transparency via POSIX-compliant APIs.

**Application.** For our multi-threaded application, we use the in-memory key-value store (dubbed MIND-KVS) from the



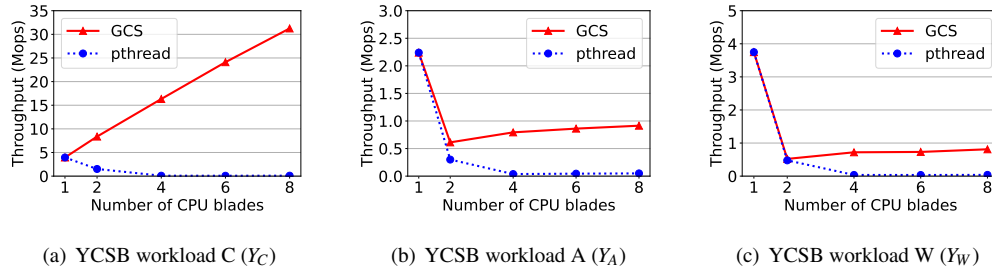


Fig. 7: **Performance scaling for MIND-KVS across  $Y_C$ ,  $Y_A$  and  $Y_W$  workloads.** GCS enables linear scaling from 1 to 8 compute blades for the read-only  $Y_C$ . For the write-only  $Y_W$ , GCS achieves the ideal scaling scenario of constant throughput with more compute blades for 2 – 8 blades, albeit with a drop from 1 to 2 blades due to the added network traffic. For the write-heavy  $Y_A$ , GCS observes a similar drop from 1 to 2 blades, but preserves throughput scaling from 2 to 8 blades. The `pthread_rwlock` in contrast, observes much lower absolute performance and poor performance scaling, due to redundant coherence transactions over the network.

MIND paper [33]. MIND implements its own key-value store since it currently lacks a network stack for communicating with external clients, precluding the deployment of traditional in-memory key-value stores [48, 49]. MIND-KVS employs a hash table where each hash bucket is protected against concurrent accesses by a fine-grained `pthread_rwlock` reader-writer lock. Since `pthread_rwlock` does not support explicitly specifying the shared state protected by the lock, GCS infers it by tracking the accessed shared state in its critical section (§3.2).

**Workloads.** Our evaluation employs various YCSB workloads [50], including YCSB workloads A (100% read, denoted as  $Y_A$ ), B (50% read and 50% update, denoted as  $Y_C$ ) and a customized workload W (100% update, denoted as  $Y_W$ ) to highlight the impact of writer-writer synchronizations. We use the default 1KB value size and 0.99 skewness parameters for YCSB workloads.

### 5.1 Performance for Real-World Workloads

Fig. 7 shows the throughput scaling of MIND-KVS for both the layered design and GCS with an increasing number of CPU blades. Each CPU blade hosts 10 concurrent worker threads that continuously run queries from the YCSB workload on MIND-KVS. We find that GCS enables linear scaling for MIND-KVS for the read-only  $Y_C$ , achieving 31.2 Mops throughput at 8 blades —  $331\times$  higher compared to the layered `pthread_rwlock` design! GCS’s high throughput is primarily due to its ability to exploit temporal locality for locks as outlined in §3.3 — since the Zipfian access pattern in YCSB is highly skewed, the most frequently accessed items and locks in MIND-KVS can simply remain cached at the compute blades. Moreover, since read locks in GCS do not require wait queues or invalidations (§3.1.1), multiple compute blades can cache the lock and data at the same time. In contrast, the native `pthread_rwlock` observes significantly worse performance since it requires writing to its lock variables even when acquiring a read lock, resulting in cache invalidations over the network.

For write-only workloads, the best-case scenario for any reader-writer lock is to maintain constant throughput as the

number of contending threads increases, since only one writer can hold a lock at a given point in time. While GCS observes maintains nearly constant throughput for the write-only  $Y_W$  workload from 2 to 8 blades — even enabling scaling for the 50% read-50% write  $Y_A$  workload — both GCS and `pthread_rwlock` observe a sharp performance drop moving from 1 to 2 blades. This is primarily because with a single compute blade, the frequently accessed data and their corresponding locks can be cached at the blade with no invalidations from other blades. In contrast, even with just two blades, both `pthread_rwlock` and GCS observe data and lock invalidations, triggering overheads due to added network communications. However, we note that the significantly reduced number of coherence transactions due to GCS’s spatial and temporal generalizations permit both higher absolute throughput —  $19\times$  and  $22\times$  for  $Y_A$  and  $Y_W$ , respectively — and better performance scaling relative to the native `pthread_rwlock`.

*Key takeaway:* GCS observes better absolute performance as well as performance scaling relative to traditional locks layered atop cache-coherence substrates, due to a combination of reduced cache-coherence transactions in its generalized cache coherence (§3.1) and optimizations adapted from traditional cache-coherence protocols (§3.3).

### 5.2 Understanding GCS’s Performance

We now break down how the optimizations listed in §3.3 lead to GCS’s performance gains. To this end, we compare the latency and throughput for three schemes: (1) GCS with all of the optimizations enabled, (2) GCS without the optimization that allows it to combine lock acquisition with data fetch (dubbed *w/o combined data opt* in figures), and, (3) GCS without the optimization that leverages temporal locality of locks and their associated data (dubbed *w/o locality opt* in figures). Our experimental setup employs multiple workers to continuously generate a sequence of lock acquisition, associated data access, and lock release requests. For scheme (2), the data fetch is triggered by MIND’s cache-coherence protocol, while for scheme (3), the lock and its associated data are evicted once the lock is released. We vary lock contention

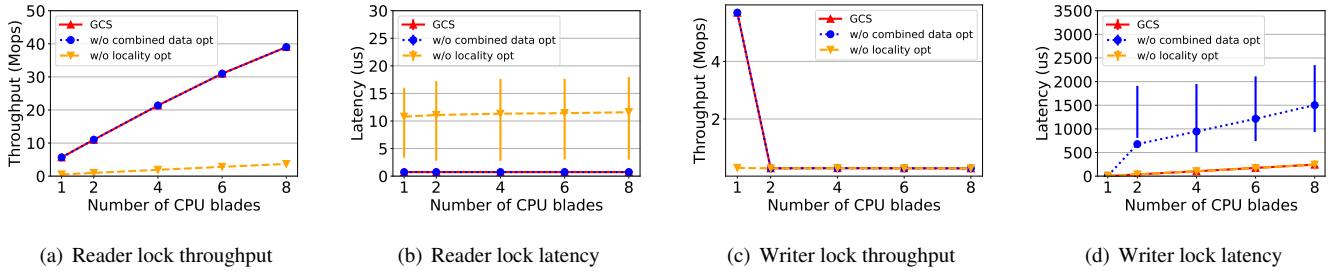


Fig. 8: **Understanding the contributions of GCS optimizations to inter-blade scaling.** GCS’s locality optimization significantly improves throughput and latency for reader-reader contentions, enabling linear scaling with the number of compute blades. Without the locality optimization, GCS reader lock throughput drops by  $\sim 11\times$ , while latency increases by  $\sim 9\times$  across all configurations. GCS’s combined data/lock acquisition optimization enables similar gains for writer-writer contentions: GCS writer lock scales near-perfectly with the number of CPU blades. Without the combined data/lock acquisition optimization, GCS writer lock throughput drops by  $6.2 - 19.5\times$ , while latency increases by  $54\% - 85\%$  across all configurations (except with 1 blade). Whiskers in (b, d) mark  $1.5\times$  the interquartile range.

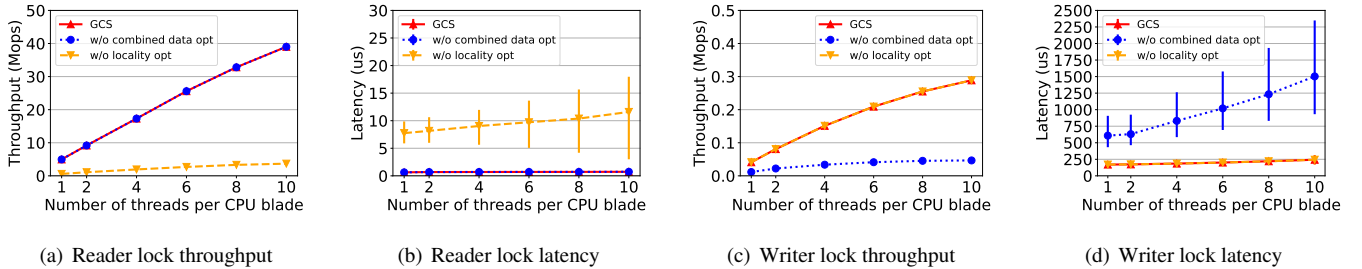


Fig. 9: **Understanding the contributions of GCS optimizations to intra-blade scaling.** As with inter-blade scaling, GCS’s locality and combined lock/data acquisition optimizations significantly improves throughput and latency for reader-reader and writer-writer contentions, respectively. Whiskers in (b, d) mark  $1.5\times$  the interquartile range.

along two dimensions — the number of CPU blades (with 10 threads per blade) to capture inter-blade scaling, and the number of threads per blade (across a fixed 8 CPU blades) to capture intra-blade scaling. For both setups, the  $i^{th}$  thread on any blade attempts to acquire the same lock, *e.g.*, in a setup with 8 compute blades and 10 threads per blade, the  $1^{st}$  thread on every blade access lock#1 and its associated data, the  $2^{nd}$  thread on every blade access lock#2, and so on. The number of locks, therefore, is always equal to the number of threads per blade in our setup. We use a shared state size of 1KB and a critical section that simply accesses the data once — we defer a study of the impact of these parameters to §5.3.

**Inter-blade scaling.** Clearly, without the temporal locality optimization, GCS with multiple readers observes much lower absolute throughput as well as performance scaling with multiple blades, since each lock acquisition must access the directory over the network (Fig. 8(a) and 8(b)). In contrast, both GCS and GCS without combined data and lock acquisition achieve much higher absolute throughput, near-linear throughput scaling, and low latency, since all lock acquisitions (except the first) and releases are served locally at the compute blade. The absence of writers means that no cached data or lock is ever invalidated. The scaling is linear even without combined data/lock acquisition since cache coherence for the data ensures that it remains in the cache after the first access.

For writer locks (Fig. 8(c) and 8(d)), the throughput de-

creases sharply from one blade to two blades, both with and without the combined data fetch optimization. As described in §5.1, this is because two or more compute blades necessitate network communications due to invalidations from other writers. As the number of blades increases from 2 to 8, GCS maintains a constant writer lock throughput ( $\sim 0.3$  Mops) regardless of contention, with a linearly increasing latency. Again, as noted in §5.1, this is the ideal performance for any reader-writer lock, since only one writer can hold a lock at any point in time — as the number of writers (blades) increases, each waiter must wait longer, with a constant throughput across all writers. Even without the combined data and lock acquisition optimization, GCS maintains the constant throughput and linearly increasing latency. However, there is a  $\sim 6\times$  reduction in throughput ( $\sim 0.05$  Mops) and increase in latency relative to GCS with the optimization, since lock and data fetch must now occur over two sequential cache-coherence transactions. Note that locality optimization has no effect on writer-writer contentions since the lock and data are forcibly invalidated over the network by another writer (on a different blade) after every acquisition. Finally, we note that the absolute latency for acquiring a writer lock is significantly higher than that for acquiring a reader lock; this is primarily because, unlike reader lock, acquiring a writer lock requires the thread to wait in the queue until the previous writer explicitly releases the lock. Combined with additional network delays for lock acquisition and queue transfers, this results in

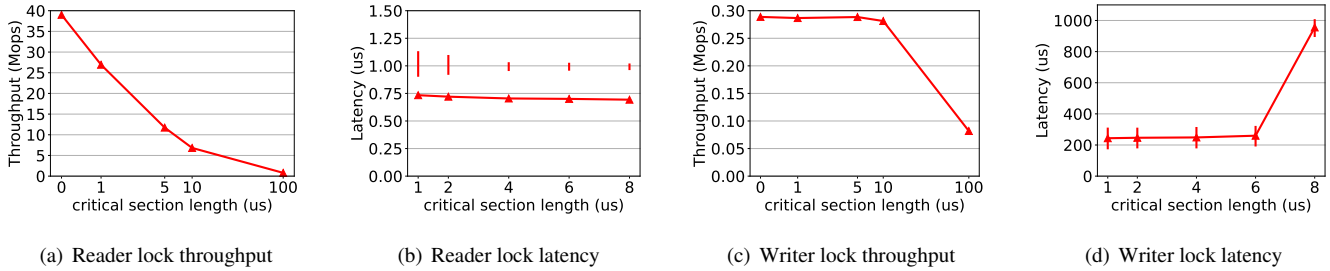


Fig. 10: **Impact of critical section length on lock performance.** Reader lock throughput and latency variability decreases as critical section length increases. Writer lock throughput and latency is unaffected by critical section length up to 10us, but observes reduced performance at 100us due to increased waiting time for contending writers. Whiskers in (b, d) mark  $1.5\times$  the interquartile range.

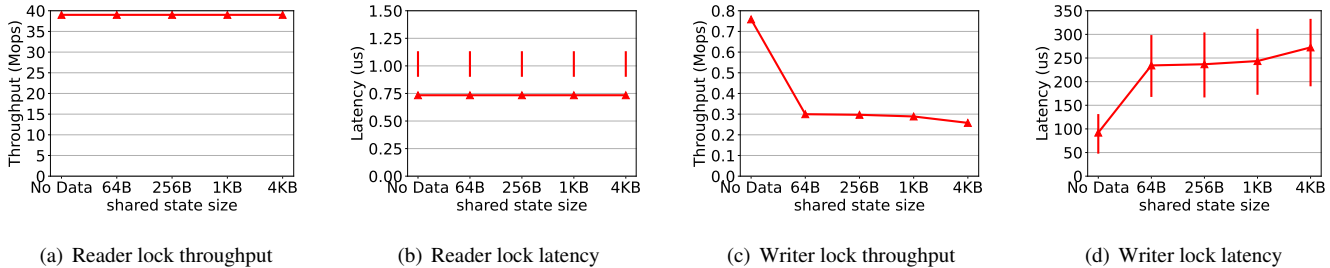


Fig. 11: **Impact of shared state size on lock performance.** Reader lock performance is unaffected by the shared state size due to GCS’s locality optimization. Writer locks observe a drop in performance from 0B (No Data) to 64B since due to added network traffic. We also note a gentle decline in performance from 1KB to 4KB due to queuing at the RDMA NIC PUs. Whiskers in (b, d) mark  $1.5\times$  the interquartile range.

higher latencies.

*Key takeaway:* For the inter-blade setup, GCS’s locality optimization significantly improves throughput, latency, and performance scaling for reader-reader contentions, while its combined data/lock acquisition optimization does the same for writer-writer contentions.

**Intra-blade scaling.** As expected, the throughput for compared schemes scales linearly with the number of threads since each thread contends for a separate lock (Fig. 9(a) and 9(b)). Also, the performance trends across different compared schemes are nearly identical to those for inter-blade scaling — our locality optimization permits near-linear scaling with the number of threads per blade, while GCS without the optimization observes lower throughput, higher latency, and worse scaling since they must issue requests over the network for every lock acquisition and release.

Similar to reader locks, while writer lock throughput increases linearly with the number of threads per compute blade, the lock acquisition latency also increases slightly (Fig. 9(c) and 9(d)); we found the root cause behind this to be increased queuing at the RDMA NIC processing units (PUs); similar observations of RDMA NIC PU saturation at high request rates and large requests have been reported in prior work [51]. We believe future RDMA NICs with more efficient PUs may eliminate these bottlenecks. Again, the trends across schemes remain similar to inter-blade scaling: the combined lock/data acquisition significantly improves both absolute performance ( $3.7\times$  to  $6.2\times$  higher throughput,  $71\% - 85\%$  lower average latency) and performance scaling by reducing contention.

*Key takeaway:* The intra-blade setup observes similar benefits from GCS’s locality and combined data/lock acquisition optimizations. While reader performance scales linearly with the number of threads per blade, writer performance scales sub-linearly due to RDMA NIC PU saturation.

### 5.3 Temporal and Spatial Generalization

We now measure how temporal and spatial generalization impact GCS’s performance. We use the same setup and workload from §5.2, but vary the critical section duration and the shared state size across 8 CPU blades, 10 threads per blade. We fix the shared state size to 1KB when varying the critical section length, and use an empty critical section when varying the shared state size.

**Impact of temporal generalization.** As expected, the reader lock throughput decreases proportionately to the length of the critical section, since the locks are held longer (Fig. 10(a) and 10(b)). Although the average acquisition latency remains constant across all critical section lengths, we find that the variability in latency decreases as the critical section length increases. Since the locks and the corresponding data are cached at all the compute blades when there are only readers, there is little to no network traffic; the decreased latency variability is primarily due to reduced contention for accessing the cached locks and data at the compute blades.

Both writer lock throughput and latency remain largely unaffected by critical section length up to 10us but observe sharp changes at 100us (Fig. 10(c) and 10(d)). This is because each acquisition request must wait for a long period before

the lock is released.

**Impact of spatial generalization on reader lock.** GCS’s reader lock acquisition throughput and latency remain unaffected as the shared state size increases (Fig. 11(a) and 11(b)). Again, this is because the locks and the corresponding data remain cached at compute blades when there are only readers contending for locks, ensuring that no data needs to be fetched over the network, and therefore, the shared state size does not impact performance.

There is a noticeable decrease in writer lock throughput and an increase in latency as we move from 0B to 64B (Fig. 11(c) and 11(d)), since at 0B GCS’s cache-coherence requests only need to wait for an acknowledgment from the cache directory rather than waiting for the data to be transferred from main memory or other CPU blades. This effectively reduces the wait time to half a network round-trip, resulting in lower latency and higher throughput. There is a less marked decrease in lock acquisition throughput and an increase in latency as the shared state size grows from 64B to 4KB, due to increased queuing at the RDMA NIC PUs (as noted in §5.2).

*Key takeaway:* Temporal and spatial generalization has no significant impact on reader-reader contentions, while long critical sections and larger shared states result in increased lock acquisition latencies for writer-writer contentions.

## 6 Limitations and Future Research

We outline key limitations of generalized cache coherence and GCS, along with future research directions they expose.

**Generalizing other cache-coherence protocols.** While both our generalized cache coherence and the GCS implementation of it work with directory-based MSI protocol, our design is still compatible with more complex cache-coherence protocols like MESI [42], MESIF [52], MOSI [43], and MOESI [44]. These protocols typically enable further scalability improvements by introducing additional permissions for reducing coherence traffic triggered by common-case coherence transactions. They also, however, introduce more intermediate states and more complex coherence transactions, requiring not only more careful adaptation of transactions to our generalized protocol but also more resources (*e.g.*, directory state and logic) for realizing a feasible implementation for GCS. We leave their generalization to future work.

**Generalized cache coherence on other platforms.** GCS implements generalized cache coherence on a very specific architecture for directory-based MSI coherence; many other variants of the architecture exist, including those that have distributed (partitioned) directories which may be placed closer to compute units or memory units. Moreover, our implementation focuses on a cache coherent substrate that leverages Ethernet and programmable switches; emerging high-performance interconnects like Compute eXpress Link 2.0 (CXL 2.0) [36] leverage higher throughput and lower latency PCIe, and places

cache directory at the memory devices to for rack-scale memory pooling across heterogeneous compute devices. The diversity of cache-coherence implementations in such architectures opens exciting avenues for future research for GCS.

## 7 Related Work

We now describe works related to GCS.

**Distributed shared memory.** Distributed shared memory (DSM), which exposes the memory of different servers as a globally shared address space [53–55], was a concept originally introduced nearly four decades ago. In recent years, advancements in network speeds and the emergence of remote direct memory access (RDMA) have driven renewed interest in DSM designs [34, 56–58]. Cache-coherent interconnects are at the core of enabling transparent, consistent and performant access to DSM. As a consequence, several recent works have explored leveraging the programmability and line-rate processing power of emerging network switches to provide cache coherence [33, 35, 59] at the rack scale. This has even gained significant traction in the industry, where cache coherent interconnects aim to simplify heterogeneous computing and memory pooling at the rack scale [36]. Our work on generalized cache coherence aims to improve the scalability of reader-writer synchronization by extending such existing cache coherent interconnects.

**Lock-based synchronization.** Locks are the most widely used synchronization primitive in shared memory programming and is critical to parallel programs’ performance and scalability [1–14]. Queue-based locks [4, 5] achieve constant cache-coherence cost on multi-core machines regardless of contention by ordering all waiting requestors into a queue and limiting direct communication between adjacent requestors in the queue. On NUMA architectures, memory hierarchy-aware locks further optimize cache-coherence traffic by prioritizing intra-NUMA node communication over inter-NUMA node communication [6–10]. While GCS builds on queue-based locks, hierarchical locks are orthogonal to our generalized cache coherence — indeed, we can generalize hierarchical cache-coherence protocols [60–62] to achieve similar prioritization of requestors on the same compute blade.

## 8 Conclusion

In this work, we have argued for a co-design of cache coherence and reader-writer synchronization via locks. Our driving observation is that reader-writer synchronization is essentially a generalization of cache coherence in time and space. We have demonstrated GCS as an implementation of generalized cache coherence atop disaggregated memory. Our evaluations of GCS against `pthread_rwlock` that leverages a disaggregated cache coherent substrate as a black-box show that GCS outperforms the latter in both lock acquisition/release performance as well as performance scaling for real-world applications by one to two orders of magnitude.



## Acknowledgments

This work is supported in part by NSF Awards #2112562, 2147946, 2118851, and 2047220, as well as a NetApp Faculty Fellowship.

## References

- [1] Silas Boyd-Wickizer, M. Frans Kaashoek, Robert Tappan Morris, and Nickolai Zeldovich. Non-scalable locks are dangerous. 2012.
- [2] Hugo Guiroux, Renaud Lachaize, and Vivien Quéma. Multicore locks: The case is not closed yet. In *Proceedings of the 2016 USENIX Conference on Usenix Annual Technical Conference*, USENIX ATC '16, page 649–662, USA, 2016. USENIX Association.
- [3] Tudor David, Rachid Guerraoui, and Vasileios Trigonakis. Everything you always wanted to know about synchronization but were afraid to ask. In *Proceedings of the Twenty-Fourth ACM Symposium on Operating Systems Principles*, SOSP '13, page 33–48, New York, NY, USA, 2013. Association for Computing Machinery.
- [4] John M. Mellor-Crummey and Michael L. Scott. Synchronization without contention. In *Proceedings of the Fourth International Conference on Architectural Support for Programming Languages and Operating Systems*, ASPLOS IV, page 269–278, New York, NY, USA, 1991. Association for Computing Machinery.
- [5] Travis S. Craig. Building fifo and priority-queuing spin locks from atomic swap. 1993.
- [6] David Dice, Virendra J. Marathe, and Nir Shavit. Lock cohorting: A general technique for designing numa locks. In *Proceedings of the 17th ACM SIGPLAN Symposium on Principles and Practice of Parallel Programming*, PPOPP '12, page 247–256, New York, NY, USA, 2012. Association for Computing Machinery.
- [7] Milind Chabbi, Michael Fagan, and John Mellor-Crummey. High performance locks for multi-level numa systems. In *Proceedings of the 20th ACM SIGPLAN Symposium on Principles and Practice of Parallel Programming*, PPOPP 2015, page 215–226, New York, NY, USA, 2015. Association for Computing Machinery.
- [8] Dave Dice and Alex Kogan. Compact numa-aware locks. In *Proceedings of the Fourteenth EuroSys Conference 2019*, EuroSys '19, New York, NY, USA, 2019. Association for Computing Machinery.
- [9] Sanidhya Kashyap, Irina Calciu, Xiaohe Cheng, Changwoo Min, and Taesoo Kim. Scalable and practical locking with shuffling. In *Proceedings of the 27th ACM Symposium on Operating Systems Principles*, SOSP '19, page 586–599, New York, NY, USA, 2019. Association for Computing Machinery.
- [10] Rafael Lourenco de Lima Chehab, Antonio Paolillo, Diogo Behrens, Ming Fu, Hermann Härtig, and Haibo Chen. Clof: A compositional lock framework for multi-level numa systems. In *Proceedings of the ACM SIGOPS 28th Symposium on Operating Systems Principles*, SOSP '21, page 851–865, New York, NY, USA, 2021. Association for Computing Machinery.
- [11] Linux kernel brlock. <https://lwn.net/Articles/378911>, 2010.
- [12] Ran Liu, Heng Zhang, and Haibo Chen. Scalable read-mostly synchronization using passive Reader-Writer locks. In *2014 USENIX Annual Technical Conference (USENIX ATC 14)*, pages 219–230, Philadelphia, PA, June 2014. USENIX Association.
- [13] Irina Calciu, Dave Dice, Yossi Lev, Victor Luchangco, Virendra J. Marathe, and Nir Shavit. Numa-aware reader-writer locks. *SIGPLAN Not.*, 48(8):157–166, feb 2013.
- [14] Dave Dice and Alex Kogan. BRAVO—Biased locking for Reader-Writer locks. In *2019 USENIX Annual Technical Conference (USENIX ATC 19)*, pages 315–328, Renton, WA, July 2019. USENIX Association.
- [15] C++ Atomic Primitives. <http://en.cppreference.com/w/cpp/atomic/atomic>.
- [16] Java Atomic Primitives. <https://docs.oracle.com/javase/7/docs/api/java/util/concurrent/atomic/package-summary.html>.
- [17] Go Atomic Primitives. <https://golang.org/pkg/sync/atomic/>.
- [18] Shigeru Shiratake. Scaling and performance challenges of future dram. In *International Memory Workshop (IMW)*, 2020.
- [19] High Throughput Computing Data Center Architecture. [http://www.huawei.com/ilink/en/download/HW\\_349607](http://www.huawei.com/ilink/en/download/HW_349607).
- [20] The Machine: A new kind of computer. <https://www.hpl.hp.com/research/systems-research/themachine/>.
- [21] Intel Rack Scale Design: Just what is it? <https://www.datacenterdynamics.com/en/opinions/intel-rack-scale-design-just-what-is-it/>.
- [22] Facebook’s Disaggregated Racks Strategy Provides an Early Glimpse into Next Gen Cloud Computing Data Center Infrastructures. <https://dcig.com/2015/01/facebooks-disaggregated-racks-strategy-provides-early-glimpse-into-next-gen-cloud-computing-data-center-infrastructures/>.

- [23] Rack-scale Computing. <https://www.microsoft.com/en-us/research/project/rack-scale-computing/>.
- [24] Krste Asanović. FireBox: A Hardware Building Block for 2020 Warehouse-Scale Computers. 2014.
- [25] Stanko Novakovic, Alexandros Daglis, Edouard Bugnion, Babak Falsafi, and Boris Grot. Scale-out NUMA. In *ASPLOS*, 2014.
- [26] Ling Liu, Wenqi Cao, Semih Sahin, Qi Zhang, Juhyun Bae, and Yanzhao Wu. Memory Disaggregation: Research Problems and Opportunities. In *ICDCS*, 2019.
- [27] Kevin Lim, Jichuan Chang, Trevor Mudge, Parthasarathy Ranganathan, Steven K. Reinhardt, and Thomas F. Wenisch. Disaggregated Memory for Expansion and Sharing in Blade Servers. In *ISCA*, 2009.
- [28] K. Lim, Y. Turner, J. R. Santos, A. AuYoung, J. Chang, P. Ranganathan, and T. F. Wenisch. System-level Implications of Disaggregated Memory. In *HPCA*, 2012.
- [29] Ahmad Samih, Ren Wang, Christian Maciocco, Mazen Kharbutli, and Yan Solihin. *Collaborative Memories in Clusters: Opportunities and Challenges*. 2014.
- [30] Juncheng Gu, Youngmoon Lee, Yiwen Zhang, Mosharaf Chowdhury, and Kang G. Shin. Efficient Memory Disaggregation with Infiniswap. In *NSDI*, 2017.
- [31] Emmanuel Amaro, Christopher Branner-Augmon, Zhihong Luo, Amy Ousterhout, Marcos K. Aguilera, Aurojit Panda, Sylvia Ratnasamy, and Scott Shenker. Can Far Memory Improve Job Throughput? In *EuroSys*, 2020.
- [32] Yizhou Shan, Yutong Huang, Yilun Chen, and Yiyang Zhang. LegoOS: A Disseminated, Distributed OS for Hardware Resource Disaggregation. In *OSDI*, 2018.
- [33] Seung-seob Lee, Yanpeng Yu, Yupeng Tang, Anurag Khandelwal, Lin Zhong, and Abhishek Bhattacharjee. Mind: In-network memory management for disaggregated data centers. In *Proceedings of the ACM SIGOPS 28th Symposium on Operating Systems Principles, SOSP '21*, page 488–504, New York, NY, USA, 2021. Association for Computing Machinery.
- [34] Qingchao Cai, Wentian Guo, Hao Zhang, Divyakant Agrawal, Gang Chen, Beng Chin Ooi, Kian-Lee Tan, Yong Meng Teo, and Sheng Wang. Efficient Distributed Memory Management with RDMA and Caching. *Proc. VLDB Endow.*, 11(11):1604–1617, July 2018.
- [35] Qing Wang, Youyou Lu, Erci Xu, Junru Li, Youmin Chen, and Jiwu Shu. Concordia: Distributed Shared Memory with In-Network Cache Coherence. In *FAST*, 2021.
- [36] Compute Express Link. <https://www.computeexpresslink.org>.
- [37] Ananth Devulapalli. Distributed queue-based locking using advanced network features. In *ICPP*, 2005.
- [38] Dong Young Yoon, Mosharaf Chowdhury, and Barzan Mozafari. Distributed lock management with rdma: Decentralization without starvation. In *SIGMOD*, 2018.
- [39] Xingda Wei, Jiaxin Shi, Yanzhe Chen, Rong Chen, and Haibo Chen. Fast in-memory transaction processing using rdma and htm. In *SOSP*, 2015.
- [40] Zhuolong Yu, Yiwen Zhang, Vladimir Bravermann, Mosharaf Chowdhury, and Xin Jin. NetLock: Fast, Centralized Lock Management Using Programmable Switches. In *SIGCOMM*, 2009.
- [41] MSI Protocol. [https://en.wikipedia.org/wiki/MSI\\_protocol](https://en.wikipedia.org/wiki/MSI_protocol).
- [42] MESI Protocol. [https://en.wikipedia.org/wiki/MESI\\_protocol](https://en.wikipedia.org/wiki/MESI_protocol).
- [43] MOSI Protocol. [https://en.wikipedia.org/wiki/MOSI\\_protocol](https://en.wikipedia.org/wiki/MOSI_protocol).
- [44] MOESI Protocol. [https://en.wikipedia.org/wiki/MOESI\\_protocol](https://en.wikipedia.org/wiki/MOESI_protocol).
- [45] MIND github repository. <https://github.com/Yale-NeRD/mind>.
- [46] Posix thread library reader-writer lock. [https://linux.die.net/man/3/pthread\\_rwlock\\_init](https://linux.die.net/man/3/pthread_rwlock_init).
- [47] Hubertus Franke, Rusty Russell, and Matthew Kirkwood. Fuss, futexes and furwocks: Fast userlevel locking in linux. 01 2002.
- [48] Redis. <https://redis.com/>.
- [49] MemCached. <http://www.memcached.org>.
- [50] Brian F. Cooper, Adam Silberstein, Erwin Tam, Raghu Ramakrishnan, and Russell Sears. Benchmarking Cloud Serving Systems with YCSB. In *Proceedings of the 1st ACM Symposium on Cloud Computing, SoCC '10*, page 143–154, New York, NY, USA, 2010. Association for Computing Machinery.
- [51] Stanko Novakovic, Yizhou Shan, Aasheesh Kolli, Michael Cui, Yiyang Zhang, Haggai Eran, Boris Pismenny, Liran Liss, Michael Wei, Dan Tsafirir, and Marcos Aguilera. Storm: A Fast Transactional Dataplane for Remote Data Structures. In *SYSTOR*, page 97–108, 2019.

- [52] MESIF Protocol. [https://en.wikipedia.org/wiki/MESIF\\_protocol](https://en.wikipedia.org/wiki/MESIF_protocol).
- [53] Kai Li and Paul Hudak. Memory coherence in shared virtual memory systems. *ACM Trans. Comput. Syst.*, 7(4):321–359, nov 1989.
- [54] Brian N. Bershad, Matthew J. Zekauskas, and Wayne A. Sawdon. The Midway Distributed Shared Memory System. Technical report, 1993.
- [55] Daniel Lenoski, James Laudon, Kouros Gharachorloo, Wolf-Dietrich Weber, Anoop Gupta, John Hennessy, Mark Horowitz, and Monica S. Lam. The Stanford Dash Multiprocessor. *Computer*, 1992.
- [56] Jacob Nelson, Brandon Holt, Brandon Myers, Preston Briggs, Luis Ceze, Simon Kahan, and Mark Oskin. Latency-Tolerant Software Distributed Shared Memory. In *ATC*, 2015.
- [57] C. Gordon Bell and Ike Nassi. Revisiting scalable coherent shared memory. *Computer*, 51(1):40–49, 2018.
- [58] Aleksandar Dragojević, Dushyanth Narayanan, Orion Hodson, and Miguel Castro. FaRM: Fast Remote Memory. In *NSDI*, 2014.
- [59] Jialin Li, Jacob Nelson, Ellis Michael, Xin Jin, and Dan R. K. Ports. Pegasus: Tolerating Skewed Workloads in Distributed Storage with In-Network Coherence Directories. In *OSDI*, 2020.
- [60] Nicolai Oswald, Vijay Nagarajan, and Daniel J. Sorin. Hieragen: Automated generation of concurrent, hierarchical cache coherence protocols. In *ISCA*, 2020.
- [61] Opeoluwa Matthews and Daniel J. Sorin. Architecting hierarchical coherence protocols for push-button parametric verification. In *MICRO*, 2017.
- [62] Joonwon Choi et al. *Structural design and proof of hierarchical cache-coherence protocols*. PhD thesis, Massachusetts Institute of Technology, 2021.